Acta Oceanol. Sin., 2014, Vol. 33, No. 11, P. 90–101
DOI: 10.1007/s13131-014-0558-7
http://www.hyxb.org.cn
E-mail: hyxbe@263.net

An upper ocean response to Typhoon Bolaven analyzed with Argo profiling floats

LIU Zenghong[1,2*], XU Jianping[1,2], SUN Chaohui[1], WU Xiaofen[1]

[1] State Key Laboratory Satellite Ocean Environment Dynamics, Second Institute of Oceanography, State Oceanic Administration, Hangzhou 310012, China
[2] Second Institute of Oceanography, State Oceanic Administration, Hangzhou 310012, China

Received 29 October 2012; accepted 29 July 2014

Abstract

In situ observations from Argo profiling floats combined with satellite retrieved SST and rain rate are used to investigate an upper ocean response to Typhoon Bolaven from 20 through 29 August 2012. After the passage of Typhoon Bolaven, the deepening of mixed layer depth (MLD), and the cooling of mixed layer temperature (MLT) were observed. The changes in mixed layer salinity (MLS) showed an equivalent number of increasing and decreasing because the typhoon-induced salinity changes in the mixed layer were influenced by precipitation, evaporation, turbulent mixing and upwelling of thermocline water. The deepening of the MLD and the cooling of the MLT indicated a significant rightward bias, whereas the MLS was freshened to the left side of the typhoon track and increased on the other side. Intensive temperature and salinity profiles observed by Iridium floats make it possible to view response processes in the upper ocean after the passage of a typhoon. The cooling in the near-surface and the warming in the subsurface were observed by two Iridium floats located to the left side of the cyclonic track during the development stage of the storm, beyond the radius of maximum winds relative to the typhoon center. Water salinity increases at the base of the mixed layer and the top of the thermocline were the most obvious change observed by those two floats. On the right side of the track and near the typhoon center when the typhoon was intensified, the significant cooling from sea surface to a depth of 200×10^4 Pa, with the exception of the water at the top of the thermocline, was observed by the other Iridium float. Owing to the enhanced upwelling near the typhoon center, the water salinity in the near-surface increased noticeably. The heat pumping from the mixed layer into the thermocline induced by downwelling and the upwelling induced by the positive wind stress curl are the main causes for the different temperature and salinity variations on the different sides of the track. It seems that more time is required for the anomalies in the subsurface to be restored to pretyphoon conditions than for the anomalies in the mixed layer.

Key words: Typhoon Bolaven, Argo profiling floats, upper ocean response, ocean heat content

Citation: Liu Zenghong, Xu Jianping, Sun Chaohui, Wu Xiaofen. 2014. An upper ocean response to Typhoon Bolaven analyzed with Argo profiling floats. Acta Oceanologica Sinica, 33(11): 90–101, doi: 10.1007/s13131-014-0558-7

1 Introduction

A typhoon (tropical cyclone, hereafter TC) is one of the most extreme air-sea interactions, and its energy is mainly supplied by warm waters through a surface heat flux (Emanuel, 1986). The strong typhoon winds induce strong turbulent mixing and entrainment of cold water from below into the mixed layer (ML), which results in the cooling of the mixed layer water and deepening of the MLD (Bender et al., 1993; Ginis, 2002). Price (1981) suggested that the entrainment by turbulent mixing generated by a hurricane was responsible for 85% of the irreversible heat flux out of the ocean mixed layer, while a direct air-sea heat exchange played a minor role in the cooling. Generally, the typhoon-induced sea surface cooling can exceed 3°C, and in some cases even up to 7–11°C, within a few hundred kilometers of the typhoon center, which can persist for 1–3 weeks. The cyclonic wind stress induced by the typhoon causes cold water upwelling in a large region (about several hundred kilometers), and subsequently, the rising of the thermocline (Price, 1981). It was suggested that the MLD changes played an important role in determining the responses of sea surface temperature (SST) to the TCs (Mao et al., 2000). The cooling rate of the deep ML could be slower, which prolongs the heat transport to the atmosphere. Strong TCs usually result in the decreasing of the SST and the near-surface temperature, but the warming of the subsurface water. Upwelling caused by the positive wind stress curls in the centre of a cyclonic track, and surface heat loss to the atmosphere lead to the upper ocean cooling, though without causing subsurface warming (Park et al., 2011; Maneesha et al., 2012). In short, tropical cyclones are known to pump heat downward and drive colder water upward due to Ekman-pumping induced by strong cyclonic wind stress curl. Near the TC center, the surface water is transported outward and the cold deep water is pumped upward (upwelling). In the periphery of the storm, the surface water accumulates and weak downwelling occurs (Ginis, 2002). Emanuel (2001) proposed that the near-subsurface cooling would be restored by air-sea heat fluxes toward the pre-TC state within a few weeks after a TC passage, while the subsurface warming would persist for a longer time. The ocean's response processes to a TC includes forced and relaxation stages (Price et al., 1994). The forced stage response during the storm

Foundation item: The National Basic Research Program (973 Program) of China under contract No. 2013CB430301; the National Natural Science Foundation of China under contract No. 41206022; the Ministry of Science and Technology of China under contract No. 2012FY112300.
*Corresponding author, E-mail: liuzenghong@139.com

passage is a mainly local (depth and time dependent) response of the ocean to the strong wind stress. The forced stage baroclinic response includes ML currents of O (1 m/s) (Sanford et al., 1987) and the substantial cooling of the ML and the sea surface by vertical mixing (Black, 1983; Stramma et al., 1986; Ginis and Dikiniov, 1989). The barotropic response consists of a geostrophic current and an associated trough in a sea surface height set up almost instantaneously. The time scale of the forced stage response is the TC residence time, which is typically half a day. The relaxation stage response after a TC passage is an inherently nonlocal baroclinic response to the stress curl of the TC. The energy of wind-driven ML currents is dispersed and penetrated into the thermocline in a spreading wake of near inertial frequency internal waves (Geisler, 1970; Gill, 1984; Brooks, 1983; Shay and Elsberry, 1987; Brink, 1989), and eventually leaving behind a baroclinic geostrophic current along the TC track. The time scale of the relaxation stage response is typically 5–10 d.

Owing to the severe weather condition during the TC passage, it is very difficult to obtain in situ observations of the upper ocean. In the past, only a few in situ data obtained from airborne expendable bathythermograph (AXBT) and airborne expendable current profiler (AXCP) were used (Sanford et al., 1987; Black, 1983). D'Asaro (2003) studied the evolution of the upper ocean during the passage of Hurricane Dennis in the North Atlantic, with aircraft-deployed neutrally buoyant floats for observing the water temperature and pressure. Some time-series observations from moorings where a few hurricanes fortuitously passed were used to analyze the upper ocean responses (Dickey et al., 1998; Black and Dickey, 2008). In recent years, various satellite remote sensing data were widely used to study the upper ocean responses to TCs (e.g., Lin et al., 2003; Sun et al., 2009; Yang et al., 2010; Sun et al., 2012). As the global Argo array consisting of 3 000 profiling floats was achieved in 2007, more and more *in situ* observations of the upper ocean could be obtained by Argo floats during the passage of TCs, and used to analyze the upper ocean responses to TCs (e.g., Yang et al, 2010; Park et al., 2011; Liu et al., 2006; Liu et al., 2007; Chen et al., 2012). In particular, the Iridium communication system with the advantage of high speed transmission and two-way communication advantages are widely used, with which the Argo float could adjust its cycle time, maximum depth of high resolution profile, and so on during TCs passage. The deployments of Iridium Argo floats can carry out an intensive observing between the middle and the upper ocean, which will vastly facilitate us to further analyze the upper ocean responses to TCs.

In this paper, we use the Argo profiling data (including some Iridium Argo floats) obtained during the passage of Typhoon Bolaven, combined with the satellite retrieved data, to analyze the upper ocean response and its process.

2 Data

2.1 *Typhoon track*

Typhoon Bolaven's track data are provided by Unisys weather information systems, USA (http://weather.unisys.com), which is based on the best typhoon track data prepared by the Joint Typhoon Warning Center (JTWC). The track information includes typhoon center positions in latitude and longitude, maximum sustained winds, and a typhoon scale (according to the Saffir-Simpson Hurricane scale) every 6 h. The track of Typhoon Bolaven is shown in Fig. 1. Developed as a tropical depression in the western north Pacific (17.3°N, 141.5°E) on 20 August, Bolaven intensified near the region of 18.7°N and 139.8°E, reaching Category 1 (maximum sustained wind speed about 33.4 m/s) on 21 August. As of 28 August, Bolaven depressed as a tropical storm near the region of 34.8°N and 124.7°E.

2.2 *Sea surface winds*

The NOAA NESDIS National Climatic Data Center (NCDC) blended daily 0.25° sea surface winds (10 m height above sea level) are used to investigate the wind vector distributions for Typhoon Bolaven. This gridded data set is generated from the multiple satellite observations of DOD, NOAA, and NASA, and wind retrievals of the remote sensing systems (RSS), Inc. (http://www.remss.com) with direction from NCEP Reanalysis-2, using scientific methods such as objective analysis (OA). The data set has a global ocean coverage with a 0.25° resolution, and a daily temporal resolution. It is available at http://www.ncdc.noaa.gov/thredds/OceanWinds.html?dataset=oceanwindsdly. Note that though the data set is the product of multiple satellite observations, its wind speed under a TC is usually less than that of the maximum sustained wind speed reported by typhoon track, and a large area of missing data can still be found under a TC center.

2.3 *Satellite data*

Though the satellite remote sensing technology makes it

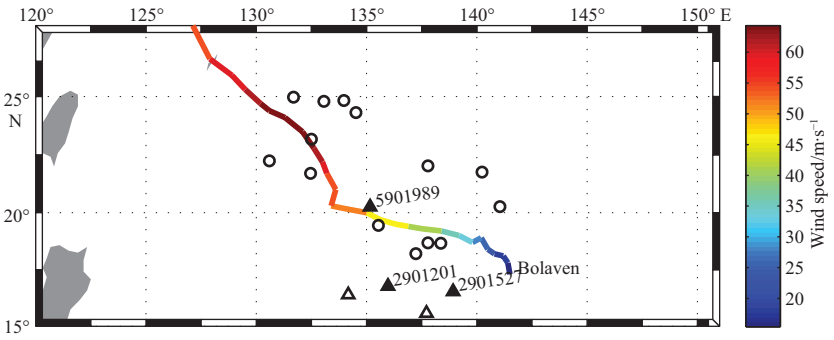

Fig.1. The track of Typhoon Bolaven and positions of nearby Argo floats. The colors indicate the maximum sustained wind speed. Black open circles indicate standard Argo floats, and black open triangles indicate Iridium Argo floats. The three selected Iridium floats in our study are marked with filled triangles.

possible to obtain widespread data such as sea surface temperature (SST), wind speed and rain rate under typhoon weather condition, in many satellite retrieved products, there is relatively large errors or missing values affected by clouds, water vapour, and strong wind speed. Therefore, the MW OI SST product provided by the remote sensing system (http://www.ssmi.com) was selected in our study. The product merged daily SST products, with a 0.25° spatial resolution retrieved from the Microwave Imager (TMI) and the Advanced Microwave Scanning Radiometer for EOS (AMSR-E). The 7th version of WindSat product including surface wind speed and rain rate from the RSS was also selected, which had the same temporal and spatial resolutions as those of the MW OI SST.

2.4 *Argo profiling data*

In order to intensively investigate the upper ocean water parameters of the typhoon origin and frequently passing region in the western north Pacific, China Argo Real-time Data Center (CARDC) (http://www.argo.org.cn) adjusted the cycle time of the operating Iridium Argo floats in this area, from the original 10 d to 2–4 d in August 2012. Those floats were installed SBE-41 CP CTD sensors, with which they were able to measure a high resolution water temperature and salinity within depths of 0–1 000×10^4 Pa, with a vertical sampling interval of 2×10^4 Pa. During the passage of Typhoon Bolaven, two Iridium floats (WMO numbers: 2901201 and 2901527) were found drifting within 300 km of the Bolaven's track, which measured nine and ten temperature and salinity profiles, respectively. For each profile, a real-time quality control had been implemented at the CARDC. Another Iridium float (WMO number: 5901989) deployed by the Japan Meteorological Agency (JMA) with a cycle time of 1 d and a maximum profiling depth of 800×10^4 Pa was also selected. To analyze the restoration period after Bolaven, more profiles were collected for the above mentioned three floats. Furthermore, the data obtained from 13 standard Argo floats (with Argos satellite communication system) and three Iridium floats were also collected during the passage of Bolaven (Fig. 1). Since each Argo float parks at a depth of about 1 000×10^4 Pa, and the period it stays on the sea surface for transmitting is less than 10 h, its drifting distance would usually be less than 20 km between two cycles. As a result, the spatial variation of the water column can be disregarded. The MLD was determined by a criterion of a temperature difference less than 0.8°C. compared to its first temperature (Kara et al., 2000). The mixed layer temperature (MLT) and the mixed layer salinity (MLS) for each Argo profile are defined as the averaged temperature and salinity in the mixed layer.

3 Results

3.1 *Ocean responses in the ML*

Figure 2 shows the statistical results of the changes of the MLD, the MLT, and the MLS observed by Argo profiles after the passage of Bolaven. It was found that most of the MLDs were deepened, with the average and maximum deepenings of about 24.5×10^4 and 53.9×10^4 Pa, respectively. All the MLTs decreased after Bolaven's passage, with the average and maximum coolings of 1.6°C. and 4.9°C., respectively. Since the changes of the MLS were affected by the processes of the precipitation, evaporation, intensified vertical mixing and thermocline upwelling, the number of the decreased MLS was equivalent to that of the increased MLS, ranging from –0.3 to 0.3. The intensified velocity shears at the base of the ML induced by the strong wind stress resulted in enhanced turbulent mixing, associated with possible downward motion arising after the passage of a typhoon, which tends to increase the MLD (Price, 1981; Shay et al., 1989; Shay et al., 1992). Through a statistical analysis, Liu et al. (2007) found that about 58.5% of the MLD was deepened after the passage of the TCs, with an average deepening of 16.1 m. The wind stress-induced vertical mixing of the upper ocean entrained the cooler waters from the thermocline below into the ML, which could lead to 81.6% of the cooling of the ML, with the mean cooling of around 1.2°C.

After Bolaven's passage, the MLD to the right side of the typhoon was deepened more clearly than that of to the left side (Fig. 3a). The average deepening to the right of the typhoon track could be up to 31.5×10^4 Pa, whereas the deepening to the left side of Bolaven was only 14.4×10^4 Pa on average. The cooling

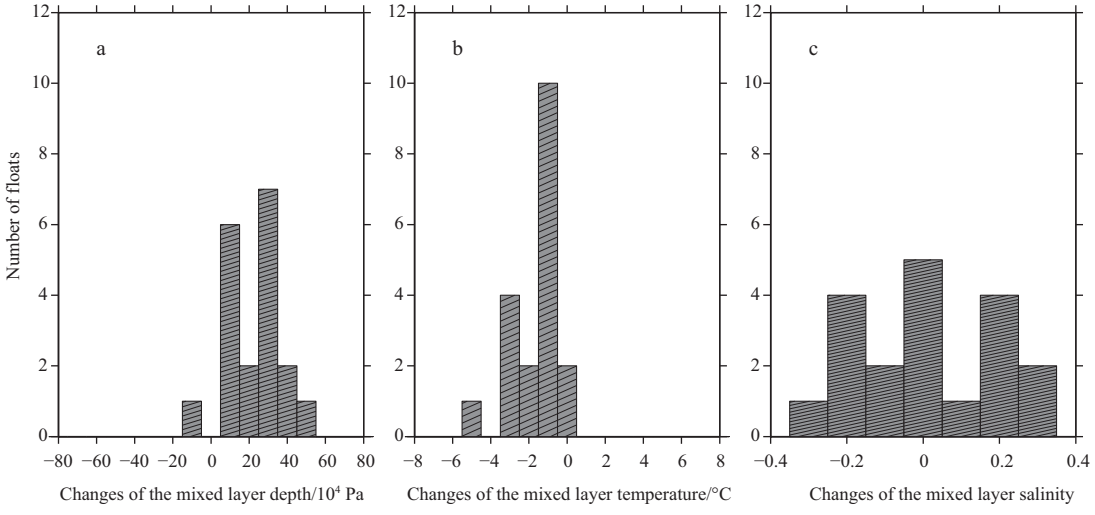

Fig.2. Histogram of MLD (a), MLT (b) and MLS (c) changes observed by Argo floats near Bolaven's track.

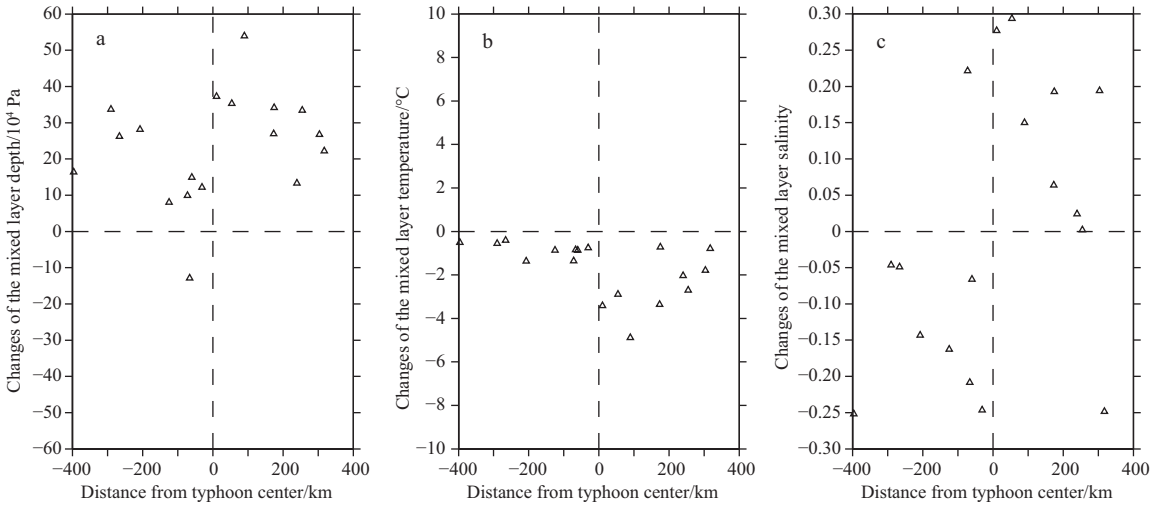

Fig.3. The changes of MLD (a), MLT (b) and MLS (c) as a function of the distance from the typhoon center observed by Argo floats. The profile to the left and right sides of the TC track is indicated by negative and positive distances, respectively.

of the MLs showed a significant characteristic of rightward bias after the passage of Balven (Fig. 3b). The MLT to the right side of Bolaven decreased by 2.5°C. on average, whereas the MLT to the left of the track decreased by only 0.8°C. This rightward bias of the cooling of the ML may be induced by the relative larger inertial currents present at the right side of the typhoon, which could enhance the turbulent mixing (D'Asaro, 2003). The MLS increased to the right of the typhoon, while it decreased to the left (Fig. 3c). It was showed that the smaller distance to the typhoon center, the larger the change in the MLS. Through a simple simulation experiment, Robertson (2003) found that the inclusion of rain as a freshwater flux into a coupled air-sea model would result in pronounced negative sea surface salinity (SSS) anomalies to the left side of the storm. He also suggested that in case of nearly symmetric fresh water flux on both sides of the storm, the significantly weaker entrainment to the left of the storm would lead to an obvious leftward bias of the SSS anomalies.

3.2 *Response processes in the ML*

To study the response processes in the ML after the passage of Bolaven, the in situ observations from three Iridium Argo floats (WMO numbers: 2901527, 2901201 and 5901989) were used. The cycle times of these floats were shortened during the passage of Bolaven via Iridium satellites. Figure 4 shows daily wind vector distribution maps from 21 to 26 August 2012, within a range of 12°–28°N and 125°–143°E. Floats 2901527 and 2901201 were located on the left periphery of the typhoon center on 21 August, whereas Float 5901989 was located in front of Bolaven's center. It likely influenced Float 5901989 on 22 August, and had a full influence on 23 August. Furthermore, the storm center was confoundedly close to the float.

Float 2901527 was located to the left side of the typhoon center (with a maximum sustained wind speed and translation speed of about 30.9 and 3.1 m/s, respectively, on 21 August), with a distance of about 266 km. Figure 4 shows the time series of temperature and salinity vertical distributions from 16 to 31 August. It can be seen that the MLD increased from 47.7×10^4 Pa before the passage of Bolaven to 70.0×10^4 Pa on 21 August, and increased to a maximum of 74.0×10^4 Pa on 23 August, then decreased gradually. The MLT decreased from 29.3°C before the passage of the typhoon on 19 August to 28.8°C on 25 August (Fig. 5a), and then was restored gradually. It can also be seen from the satellite retrieved SST near this float that the sea surface water was cooled from 29.1°C on 20 August to 28.3°C on 23 August, and subsequently warmed gradually (Fig. 6).

Figure 5b shows the time series of the salinity vertical distribution. During the passage of the typhoon, the MLS started to decrease, and decreased to a minimum of approximately 34.02 on 25 August (decreased by 0.21). After that, the MLS increased gradually, and was restored to about 34.10 on 29 August. It can be seen from the daily satellite retrieved rain rate near the float (Fig. 7a) that Typhoon Bolaven brought a relatively heavy rainfall during 20–22 August, with the average rain rate up to 1.6 mm/h, while it decreased to 0.1 mm/h on 26 August. It seemed that the heavy rainfall did not lead to an immediate freshening of water in the ML, but a period of 2–3 d was required by a full mixing to prompt a pronounced decreasing of the MLS.

Float 2901201 was also located to the left of the typhoon center (with a maximum sustained wind speed and translation speed of about 43.7 and 3.5 m/s, respectively, on 22 August), at a distance of 290 km. The nearby SST decreased rapidly from 28.9°C on 22 August to a minimum of 27.8°C on 24 August (Fig. 6). As shown by the in situ temperature distribution in Fig. 8a, the MLT started to decrease from 29°C on 22 August to a minimum value of about 28.5°C on 26–27 August. The water temperature was the lowest at a depth of 4.1×10^4 Pa on 26 August, with a value of 28.3°C. The MLD was deepened from 40.2×10^4 Pa on 20 August to 73.9×10^4 Pa on 26 August, which had a similar change as that of Float 2901527, but its deepening of the MLD would last for 2 d longer than that of Float 2901527.

The change of the MLS was different from that of Float 2901527. The MLS showed an increasing tendency with an average increasing of 0.05 from 34.08 on 20 August to 34.13 on 24 August (Fig. 8b), which could be induced by an intensified surface evaporation and a vertical mixing in the upper ocean. After that,

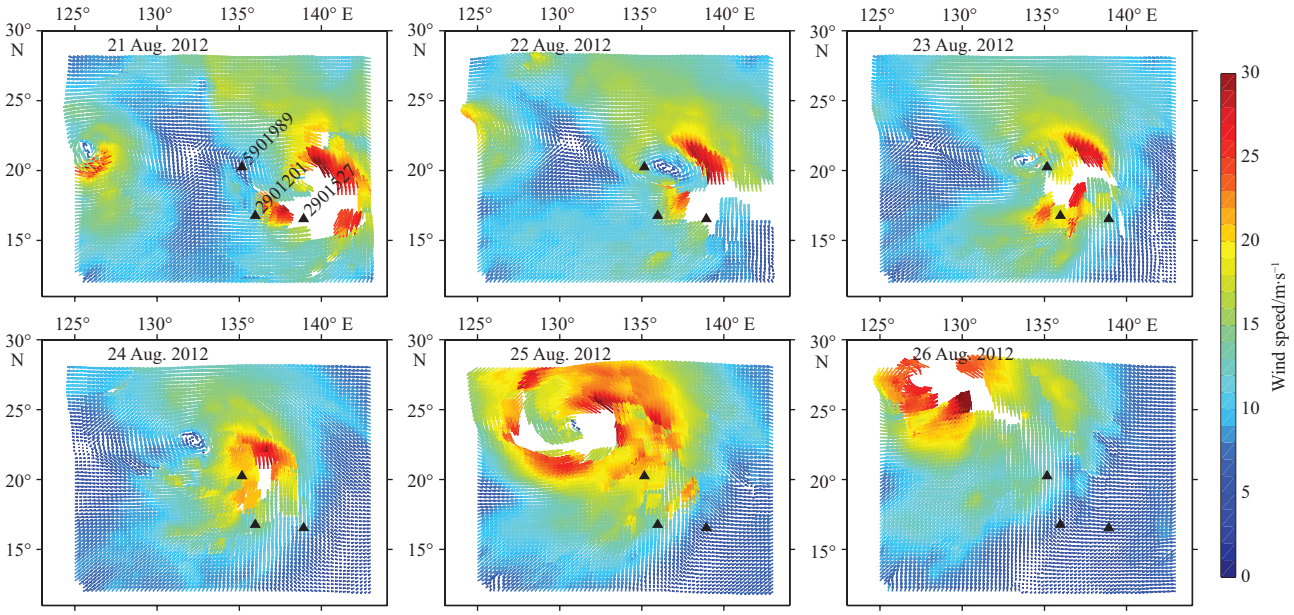

Fig.4. Daily wind vector distributions for Typhoon Bolaven during August 21–26, 2012 based on NOAA/NCDC blended daily 0.25° sea surface winds. Wind speeds are shaded by colors. The three selected Iridium profiling floats are marked with black triangles.

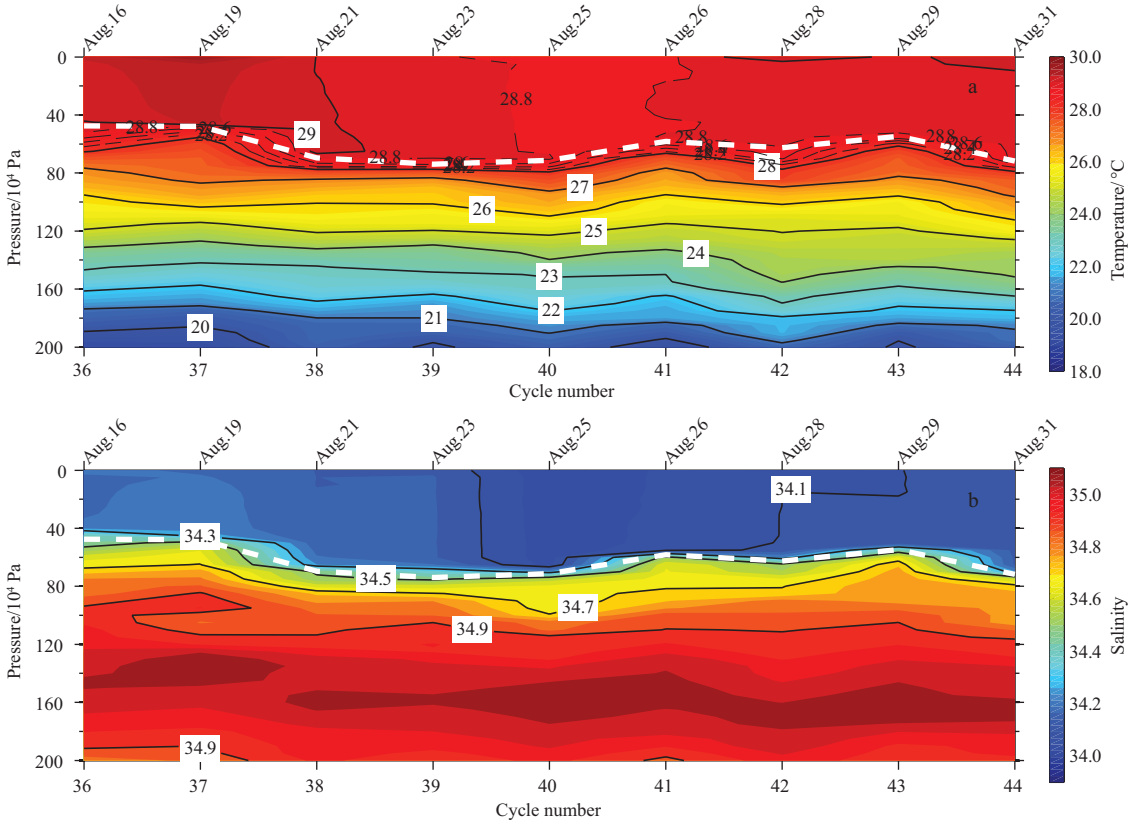

Fig.5. Vertical section of temperature (a) and salinity (b) as a function of time above 200×10⁴ Pa observed by Float 2901527 during August 16–31, 2012. The MLD is marked by the white dotted line.

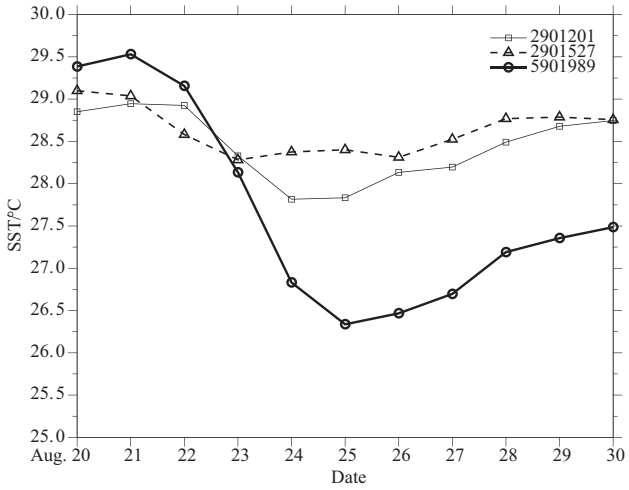

Fig.6. Daily averaged satellite retrieved SSTs in a 1°×1° box near Floats 2901201, 2901527 and 5901989 during August 20–30, 2012.

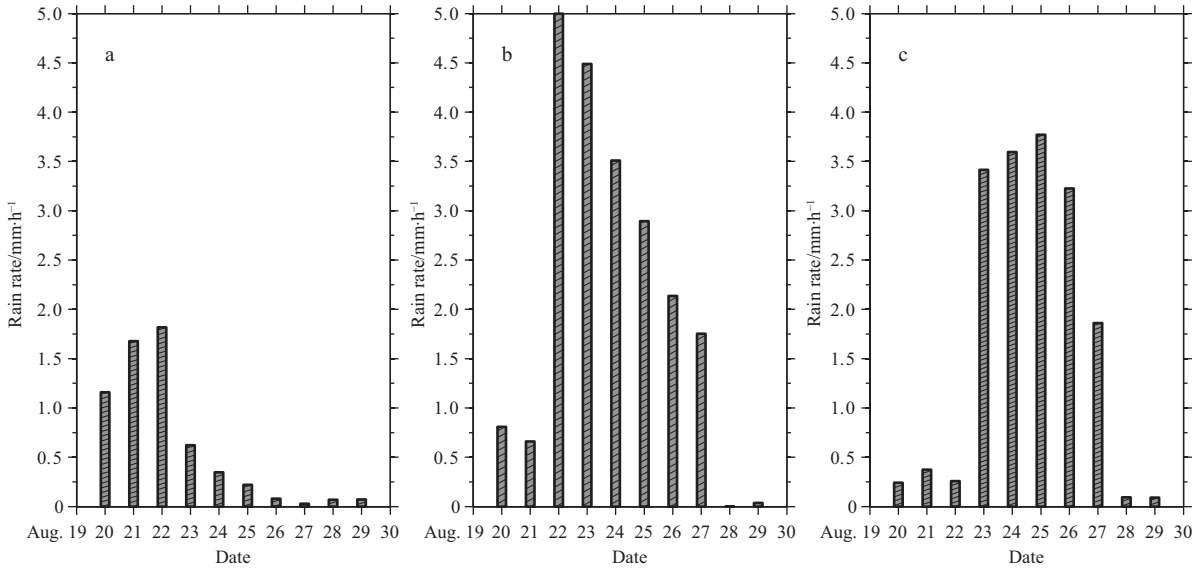

Fig.7. Daily averaged satellite retrieved rain rate in a 2°×2° box near Float 2901527 (a), 2901201 (b) and 5901989 (c) during August 20–30, 2012.

the water salinity decreased gradually. There was lower-salinity water at depths of 0–50×10^4 Pa during 26–27 August. In particular, a small strand of the lower-salinity water with a minimum of 33.70 was observed at depths between 0 and 8×10^4 Pa on 26 August, which clearly resulted from the heavy rainfall brought by Bolaven. It can be seen from Fig. 7b that the rain rate near Float 2901201 was evidently higher than that of Float 2901527 during 22–27 August, with an average value of 3.3 mm/h. However, the MLS was not freshly induced by the heavy rainfall during 22–24 August, and started to decrease until 26 August.

Float 5901989 was located to the right of the track with a distance of 55 km to the typhoon center (with a maximum sustained wind speed and translation speed of about 50.8 and 3.7 m/s, respectively, on 23 August). It observed 17 temperature and salinity profiles from 15 to 31 August. As shown by Fig. 9a, the entire ML was cooled on 23 August before the typhoon center arrived. The MLT decreased to a minimum of about 26.3°C on 26 August, and the ML was deepened to a maximum of 80.4×10^4 Pa. Subsequently, the MLT increased gradually, and the MLD decreased. The ML was deepened by 42.9×10^4 Pa and cooled by 2.9°C. compared to the observations of 22 August, which had amplitudes of changes far larger than those of Floats 2901527 and 2901201 to the left of the typhoon. It can be seen from the changes of the SST (see Fig. 6) that the cooling of the sea surface water near Float 5901989 was noticeably larger than that of the other two floats, which occurred on 22 August before the arrival of Bolaven's center. The satellite retrieved SST was only 26.3°C on 25 August, with a cooling of 3.2°C. compared to the SST on 21 August. After that, the sea surface waterwarmed up gradually, but the SST was still about 1.3°C. lower than that of the other two floats until 30 August.

The MLS observed by this float began to increase on 23 Au-

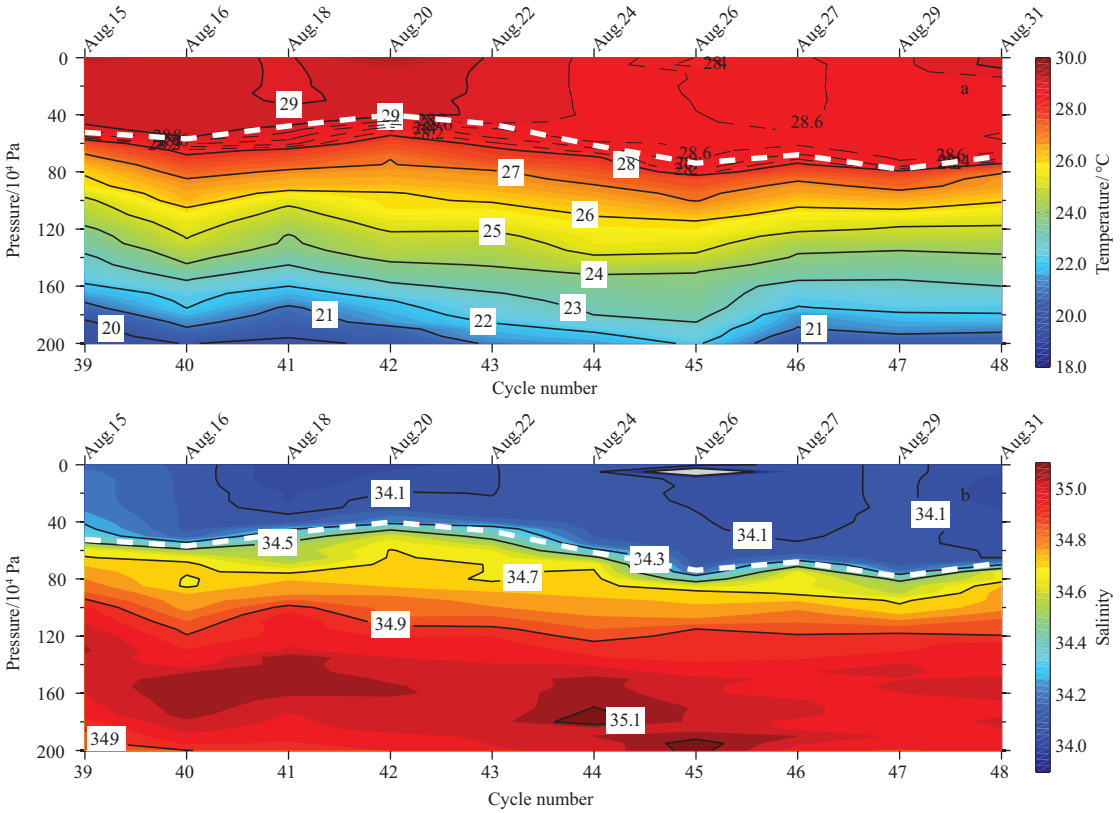

Fig.8. Vertical section of temperature (a) and salinity (b) as a function of time above 200×10⁴ Pa observed by Float 2901201 during August 15–31, 2012.

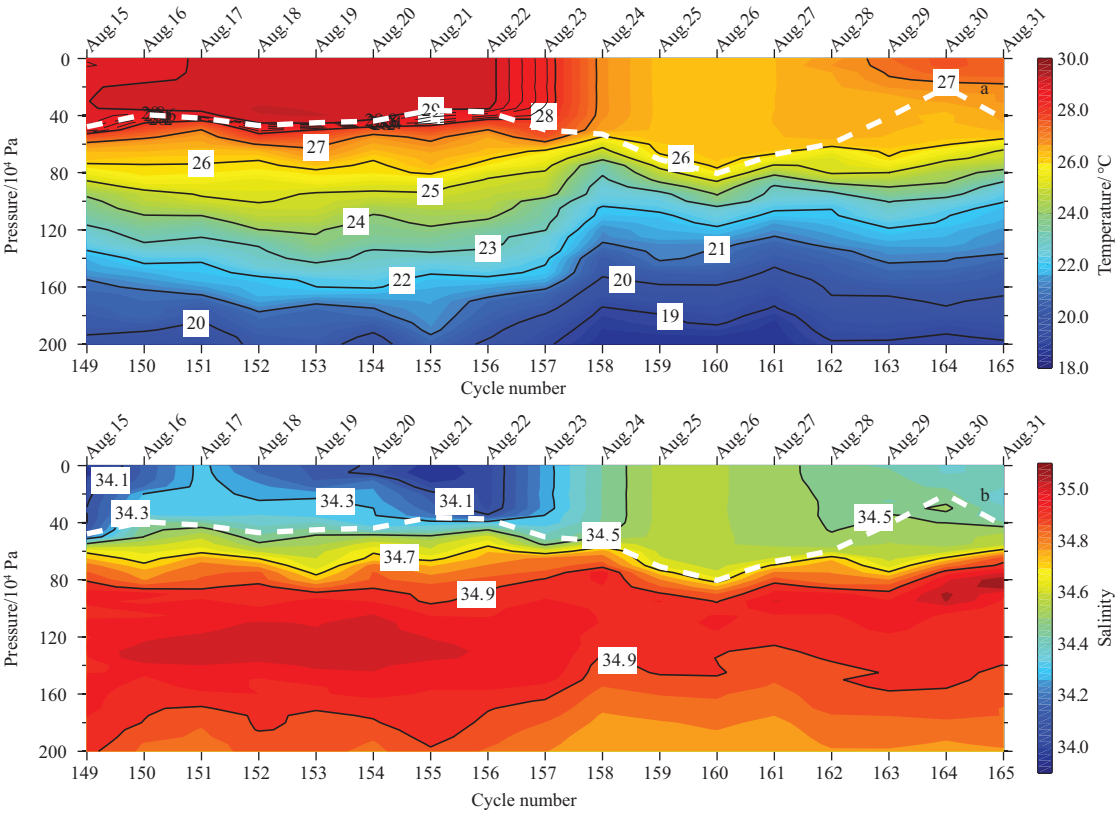

Fig.9. Vertical section of temperature (a) and salinity (b) as a function of time above 200×10⁴ Pa observed by Float 5901989 during August 15–31, 2012.

gust, and increased by 0.26 until 26 August. Subsequently, the MLS decreased gradually as the shoaling of the MLD (Fig. 9b). There was a heavy rainfall (with an average rain rate of 3.17 mm/h) from 23 to 27 August. This positive salinity feedback in the ML indicated the strong upwelling of the higher-salinity water in the thermocline into the ML, while the freshwater flux on the sea surface was insufficient to freshen the water from the entire ML.

3.3 *Variation of temperature and salinity vertical sections*

The upper ocean changes induced by the typhoon not only exist in the ML, but also occur in the thermocline. As seen from the changes of the temperature and the salinity at different depths (Fig. 10), the water temperature of Float 2901527 decreased slightly at depths between 0 and 40×10^4 Pa from 19 August (used as a reference time), and this decrease would be sustained to 1 September at least. The maximum cooling (>0.5°C) between 0 and 40×10^4 Pa occurred 4 d after the passage of Bolaven (25 August). At depths of 40×10^4–200×10^4 Pa, a wide range of warming was found, e.g., the water temperature at a depth of 60×10^4 Pa increased by around 0.5–1.5°C. immediately after the passage of the typhoon, which resulted from the downwelling and turbulent mixing associated with the increased MLD, and likewise sustained until 8 September. The water temperature at depths of 120×10^4–200×10^4 Pa was also warmed (about 0.5 –2.0°C), but it seemed that more time was required for pumping heat from the ML, and a widespread pronounced warming (>1°C) arose until 28 August. A small range of cooling was observed at about 100×10^4 Pa where the large temperature gradients are located, with a maximum cooling of 0.5°C. However, this cooling effect was quite unstable. Generally, the subsurface water was dominated by the warming tendency led by the downwelling at the typhoon periphery. It can be seen from Fig. 10b that there existed more significant freshening process at depths of 40×10^4–100×10^4 Pa than at depths above 40×10^4 Pa, with a maximum freshening of about 0.60 occurring within 2–3 d after Bolaven's passage. This freshening at the top of the thermocline could persist approximately 1 month. It likewise resulted from the enhanced vertical mixing at the base of the ML and the downwelling of the lower-salinity water from the ML into the thermocline. The water salinity below 150×10^4 Pa increased by about 0.06 due to the downwelling of the highest salinity water at about 135×10^4 Pa.

It can be seen from Fig. 11 that an average cooling of 0.5°C above 40×10^4 Pa and a wide range of warming below 40×10^4 Pa were observed by Float 2901201 after the passage of Bolaven, in which a significant warming up to 1.5°. existed at a depth of about 70×10^4 Pa and at depths between 160×10^4 and 200×10^4 Pa. The difference was that the former could persist for a longer time (from 25 August to 13 September) than the latter (from 24 to 26 August). The freshening of sea water at depths of 40×10^4–80×10^4 Pa was the most noticeable change after the passage of Bolaven on 22 August, with a maximum freshening rate of more

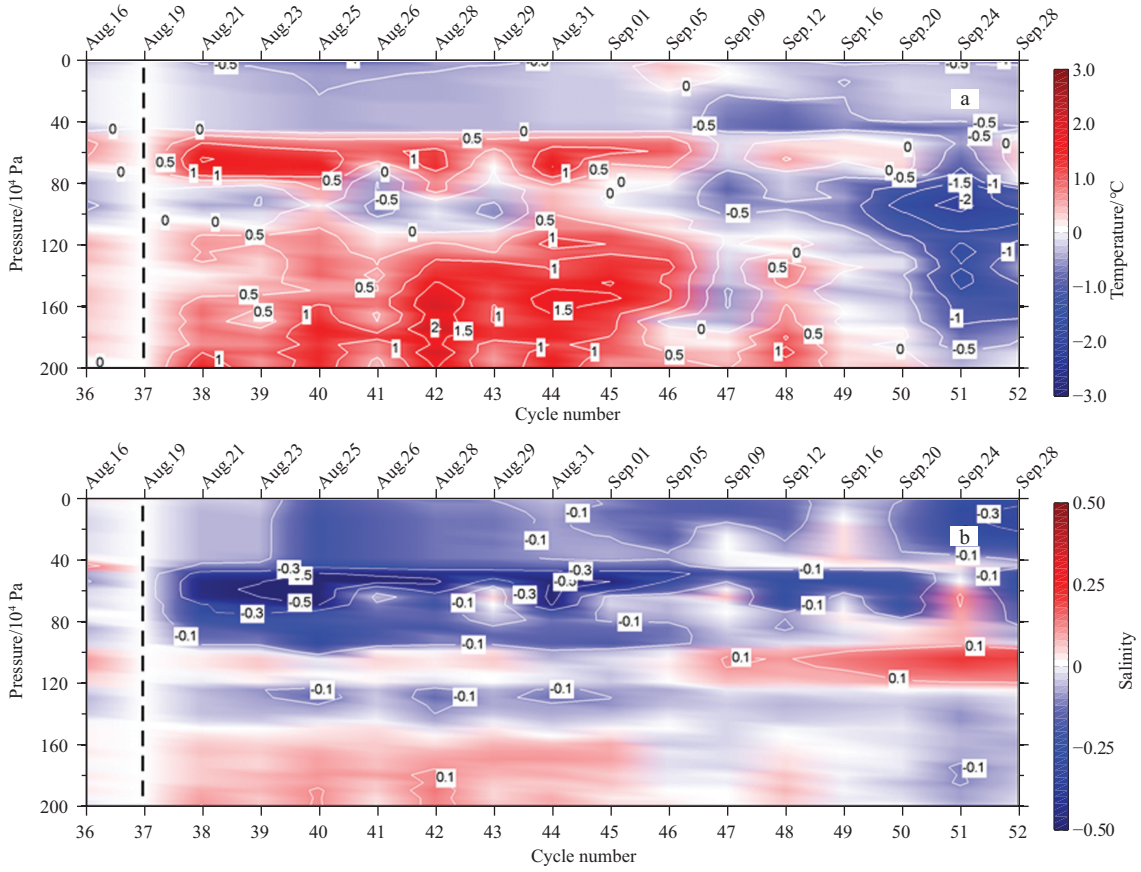

Fig.10. Vertical section of temperature (a) and salinity (b) anomalies (reference date: August 19) above 200×10^4 Pa as a function of time (August 16 to September 28) observed by Float 2901527. Black dashed line indicates a reference date.

than 50%. This freshening anomaly between the ML base and the top of the thermocline was still present 1 month after the passage of Bolaven. Clearly, the typhoon-induced downwelling and intensified entrainment of the lower-salinity water from the near-surface into the subsurface led to the significant freshening of the high-salinity water where the largest gradients in the thermocline occurred.

However, both the temperature and salinity vertical sections observed by Float 5901989 to the right side of the typhoon center presented totally different variations. As shown by Fig. 12, a wide range of cooling (comparing with that on 20 August) was observed above 200×10^4 Pa. Furthermore, except for the water between 50×10^4–80×10^4 Pa, this cooling anomaly could last for at least 1 month. A maximum cooling of up to 2.5°C. was found above 40×10^4 Pa and at depths of 125×10^4–160×10^4 Pa about 2–7 d after the passage of the typhoon. Water salinity above 45×10^4 Pa increased by up to 0.50, with a mean increasing of 0.23. This salinity anomaly tended to last for about 22 d until 14 September. Almost all the waters were freshened below 40×10^4 Pa, with an average decreasing of about 0.10, while a narrow range of saltier water could be found between 50×10^4–100×10^4 Pa. By disregarding local variations, the variations of the temperature and salinity vertical sections to the right of the typhoon were totally different from that of to the left side. The float located near the cyclonic track (about 55 km to the right side of the typhoon), the negative temperature anomaly throughout the column and positive salinity anomaly in the ML indicated strengthening of the upwelling and weakening of the turbulent mixing. Upwelling could increase the entrainment rate by reducing the ML thickness. The reduced ML thickness will contribute to an enhanced SST decrease for the same entrainment heat flux. Thus, the SST decrease above the upwelling region may be larger than in adjacent downwelling areas (Ginis, 2002). The observations in this case were consistent with the output of a numerical experiment done by Ginis (2002).

3.4 *Upper ocean heat content changes*

The upper ocean heat content changes observed by the three Iridium floats before and after the passage of Bolaven were shown in Fig. 13. Here, the upper ocean heat content is calculated as $H=\int_{200}^{0} c_p \rho T(z)\mathrm{d}z$, where $T(z)$, c_p and ρ are the temperature profile, the heat capacity and the water density, respectively. Because TCs have little influence on the ocean heat content below 200×10^4 Pa, we only calculate the heat content from 0 to 200×10^4 Pa. It can be seen from Fig. 12 that the heat contents observed by Floats 2901527 and 2901201 to the left of the cyclonic track had similar changes after the passage of the typhoon until 4 September. The heat contents did not show the decreasing tendency after 3–4 d the passage of Bolaven, and decreased until 26–27 August, restoring quickly to the pretyphoon condition around 30 August. As described in Section 3.3, the

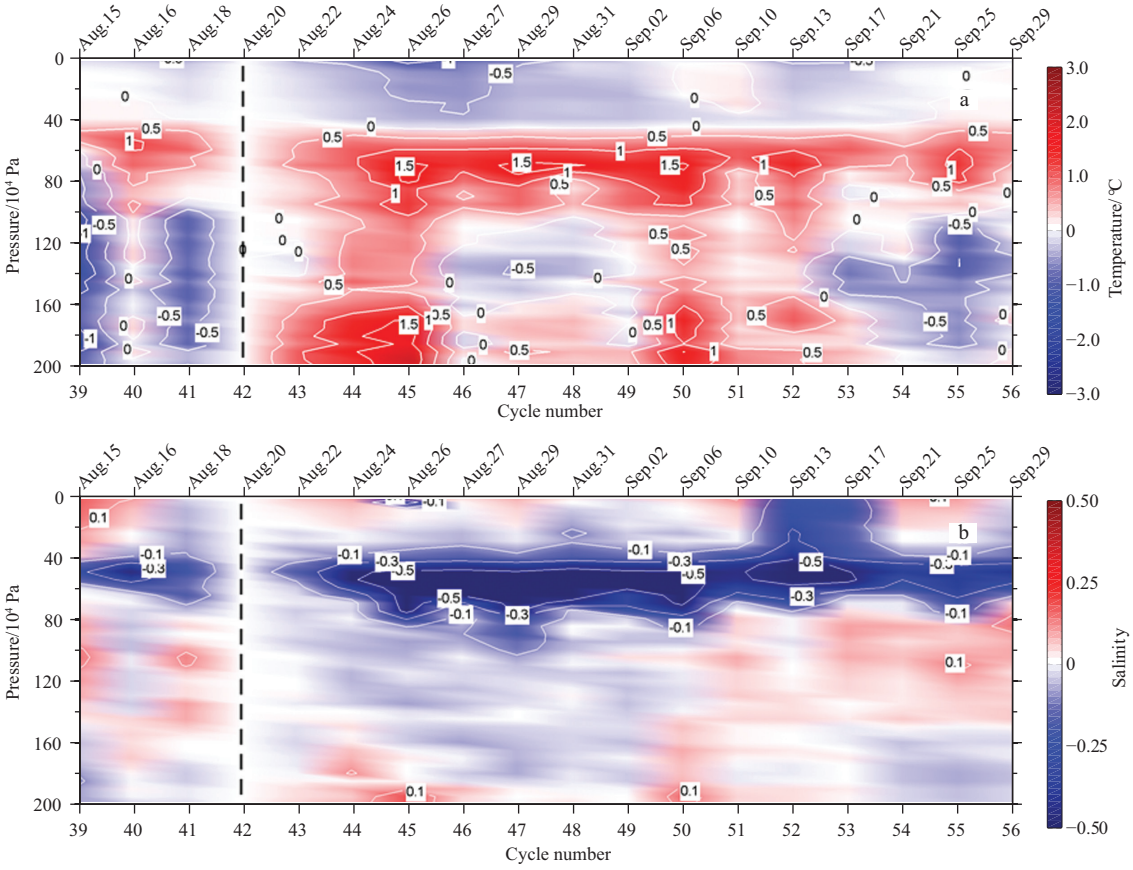

Fig.11. Vertical section of temperature (a) and salinity (b) anomalies (reference date: August 20) above 200×10^4 Pa as a function of time (August 15 to September 29) observed by Float 2901201.

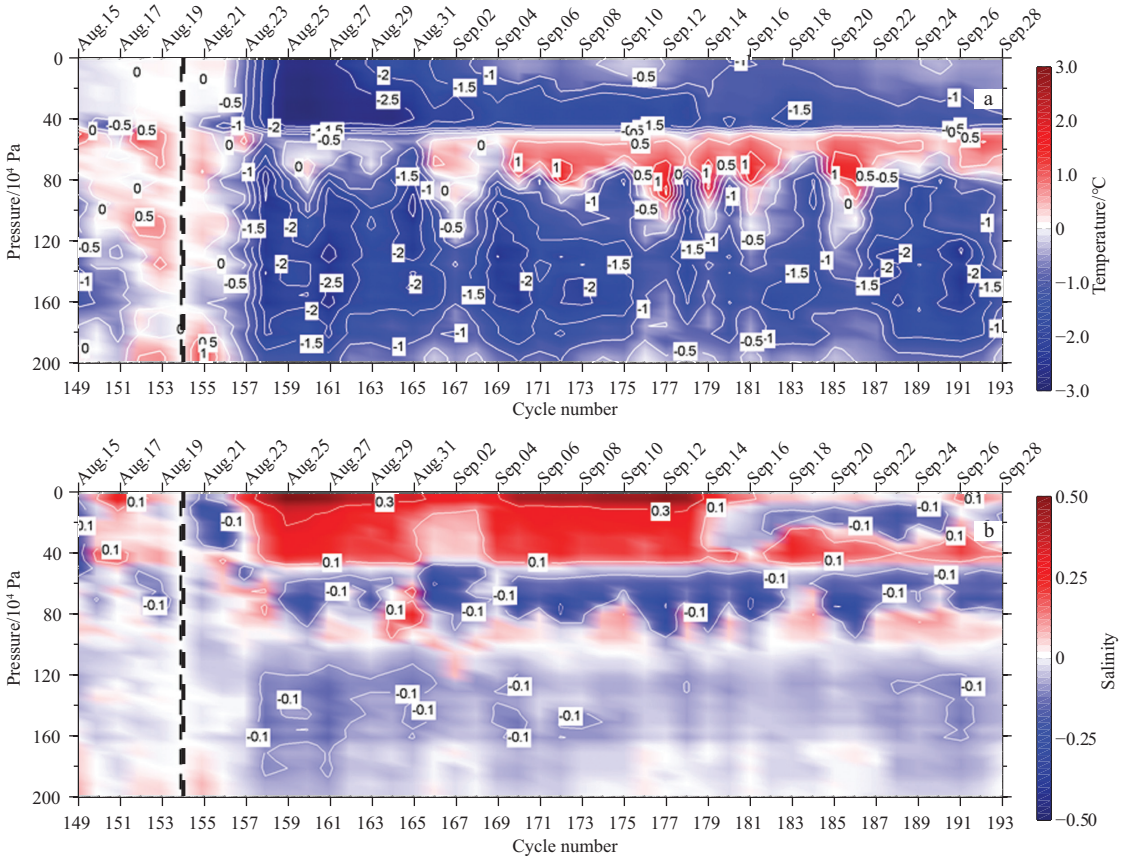

Fig.12. Vertical section of temperature (a) and salinity (b) anomalies (reference date: August 20) above 200×10⁴ Pa as a function of time (August 15 to September 28) observed by Float 5901989.

cooling in the ML induced by turbulent mixing and the subsurface warming induced by downwelling on the left side of the cyclonic track were observed after the passage of Bolaven. In those two cases, the subsurface warming contributed more to the changes of the upper ocean heat contents. By contrast, the upper ocean heat content observed by Float 5901989 decreased significantly by about 1.20 GJ/m^2 on 24 August relative to the heat content on 22 August. It seemed that 12 d was required for the upper ocean heat content to restore to the pre typhoon condition. During the passage of Bolaven near Float 5901989, the maximum sustained wind speed could be up to 51.4 m/s, which also led to a proportional increasing of the rate of transfer of heat from the ocean to the atmosphere.

During the passage of a TC, the heat transport from the upper ocean into the atmosphere could intensify the TC winds. Meanwhile, the rate of transfer of the heat is extremely dependent on the wind speed (Emanuel, 1991). Besides, the turbulent mixing induced by the TC pumped heat from the ML into the thermocline (Emanuel, 2001; Wang et al., 2012). Under TCs, especially strong TCs (greater or equal to Category 4), the near-surface cooling and the subsurface warming induced by the entrainment process (enhanced vertical mixing) can be observed, and the ocean heat content changes resulted from the near-surface cooling and the subsurface warming have comparable amplitudes (Price, 1981; D'Asaro et al., 2007). Similar results were concluded by Park et al. (2011) using the Argo profiling data in the western north Pacific, but the subsurface warming was not detected in the Argo data set under the weak TCs (less or equal to Category 3), while the near-surface cooling was still significant. Therefore, they suggested that the air-sea heat exchange and the upward vertical advection likely played a somewhat greater role in the case of the weak TCs.

4 Summary and discussion

Typhoon Bolaven was developed and passed through the western north Pacific from 20 through 29 August 2012. The Argo profiling data were used to analyze the upper ocean responses to the typhoon. The results show that most of the MLs were deepened and cooled after the passage of the typhoon, whereas equivalent numbers of the increasing and decreasing of the MLSs were observed. The deepening and cooling of the ML showed a significant rightward bias, while the MLS indicated the feature of increasing to the right of the cyclonic track and decreasing to the left side. The Iridium floats to the left of Bolaven observed around 26.2×10^4–33.7×10^4 Pa show the deepening of the ML induced by the enhanced vertical mixing process during the development stage of the storm, which could persist for 4–6 days. By contrast, the deepening and cooling of the ML were much more significant to the right side of Bolaven (about 42.9×10^4 Pa and 2.9°C, respectively) when the storm was intensified.

The upper ocean (0–200 m) on the different sides of the cy-

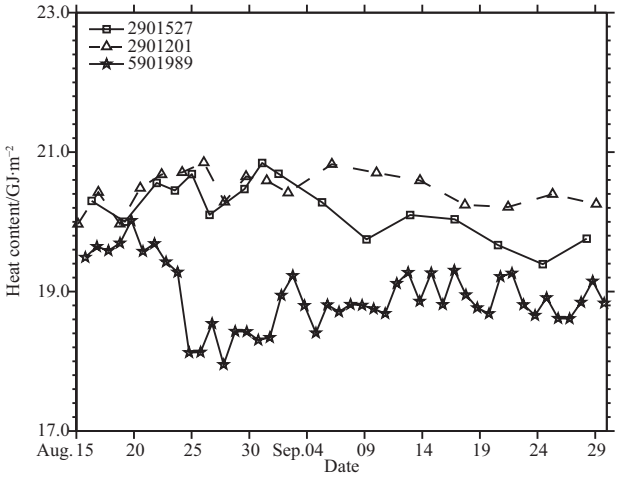

Fig.13. The upper 200 m ocean heat content estimated from three Argo floats during August 15 to September 31, 2012.

clonic track showed different variations after the passage of Bolaven. On the left side and beyond the radius of the maximum wind relative to the storm center, an average cooling of about 0.5°C above 40×10^4 Pa was observed, which could last for approximately 10 d. There existed a wide range of warming with a pronounced warming up to 1.5–2.0°C below 40×10^4 Pa led by the typhoon-induced downwelling and the turbulent mixing. The observations indicate that the subsurface warming at the top of the thermocline can persist a longer period than the cooling above 40×10^4 Pa. Meanwhile, an unstable and small range of the cooling was found at the depths where the large temperature gradients are located, which could be resulted from the enhanced vertical mixing. A significant freshening up to more than 0.50 between depths 40×10^4 to 100×10^4 Pa was the most notable change after the passage of Bolaven, which could persist for about 1 month at least. The enhanced turbulent mixing at the base of the ML and the typhoon-induced downwelling are the most important incentive for this freshening. The temperature and salinity time series observations indicate that more time is required to restore to pretyphoon conditions both for the subsurface warming and freshening than the near-surface anomalies. Beyond the radius of the maximum wind, the typhoon-induced downwelling associated with the enhanced turbulent mixing is likely to pump heat from the ML into the thermocline. A wide range of cooling which could persist at least 1 month was found above 200×10^4 Pa, except for the water between 50×10^4 and 80×10^4 Pa on the right side of the typhoon (near the typhoon center). A maximum cooling of more than 2.5°C was observed above 40×10^4 Pa and at depths of 125×10^4 to 160×10^4 Pa. The near-surface salinity above 45×10^4 Pa increased noticeably, with a maximum increasing of 0.50, which lasted for about 22 d. The water salinity tended to decrease below 40×10^4 Pa, except for the depths between 50×10^4 and 100×10^4 Pa, with a mean freshening of about 0.10. The strengthening of the upwelling and the weakening of the turbulent mixing are likely to rise the thermocline, then cause the cooling of the near-surface and subsurface water, and the increasing of the salinity in the near-surface.

Regardless of the seasonal variability of the local sea water, the processes of the upper ocean heat content changes were entirely different between the left and right sides of the typhoon. The heat content to the left of the typhoon did not tend to decrease 3–4 d after the passage of Bolaven. Though a significant decreasing was observed subsequently, it was restored immediately to the pretyphoon condition. As the winds were intensified, the rate of transfer of the heat from the ocean to the atmosphere was proportionally increased. A pronounced decreasing of the upper ocean heat content was observed by the float located to the right side of the typhoon, which could be sustain for about 12 d.

In this paper, the Argo profiling data combined with the satellite retrieved data was used to analyze the upper ocean responses to Typhoon Bolaven. In particular, the data obtained by Iridium Argo floats were used to analyze the response processes for the first time. Compared to the standard Argo float, the Iridium float has the advantages of two-way communication, faster data transmission, high resolution CTD sampling and so on, which has been widely used by the international Argo project.

Acknowledgements

The authors thank the China Argo Real-time Data Center (http://www.argo.org.cn), Unisys Weather Information Systems, USA and Remote Sensing System for providing Argo, typhoon track information and satellite remote sensing data respectively.

References

Bender M A, Ginis I, Kurihara Y. 1993. Numerical simulations of tropical cyclone-ocean interaction with a high-resolution coupled model. J Geophys Res, 98(D12): 23245–23263

Black P G. 1983. Ocean temperature changes induced by tropical cyclones [dissertation]. Pennsylvania: The Pennsylvania State University

Black W J, Dickey T D. 2008. Observations and analyses of upper ocean responses to tropical storms and hurricanes in the vicinity of Bermuda. J Geophys Res, 113: C08009

Brink K H. 1989. Observation of the response of thermocline currents to hurricane. J Phys Oceanogr, 19: 1017–1022

Brooks D A. 1983. The wake of hurricane Allen in the western Gulf of Mexico. J Phys Oceanogr, 13: 117–129

Chen X, Pan D, He X, et al. 2012. Upper ocean responses to category 5 typhoon Megi in the western north Pacific. Acta Oceanologica Sinica, 31: 51–58

D'Asaro E A. 2003. The ocean boundary layer below hurricane Dennis. J Phys Oceanogr, 33: 561–578

D'Asaro E A, Sanford T B, Niiler P P, et al. 2007. Cold wake of hurricane Frances. Geophys Res Lett, 34: L15609

Dickey T D, Frye J, McNeil D, et al. 1998. Upper-ocean temperature response to hurricane Felix as measured by the Bermuda Testbed Mooring. Mon Wea Rev, 126: 1195–1201

Emanuel K A. 1986. An air-sea interaction theory for tropical cyclones: Part I. J Atmos Sci, 43: 585–604

Emanuel K A. 1991. The theory of hurricanes. Annual Rev Fluid Mech, 23: 179–196

Emanuel K A. 2001. Contribution of tropical cyclones to meridional heat transport by the oceans. J Geophys Res, 106(14): 14771–14781

Geisler J E. 1970. Linear theory of the response of a two layer ocean to a moving hurricane. Geophys Fluid Dyn, 1: 249–272

Gill A E. 1984. On the behavior of internal waves in the wakes of storms. J Phys Oceanogr, 14: 1129–1151

Ginis I. 2002. Hurricane-ocean interactions, tropical cyclone-ocean in-

teractions, Chapter 3. In: Perrie W, ed. Atmosphere-Ocean Interactions. Advances in Fluid Mechanics Series, Volume 33. Boston, Massachusetts: WIT Press, 83–114

Ginis I, Dikinov K Z. 1989. Modelling of the Typhoon Virginia (1978) forcing on the ocean. Meteor Hydrol, 7: 53–60

Kara A B, Rochford P A, Hurlburt H E. 2000. An optimal definition for ocean mixed layer depth. J Geophys Res, 105: 16803–16821

Lin I I, Liu W T, Wu C C, et al. 2003. Satellite observations of modulation of surface winds by typhoon-induced upper ocean cooling. Geophys Res Letters, 30(3): 31

Liu Zenghong, Xu Jianping, Zhu Bokang, et al. 2006. The upper ocean response to tropical cyclones in the northwestern Pacific during 2001–2004 by Argo data. Chinese Journal of Oceanology and Limnology (in Chinese), 25(2): 123–131

Liu Z, Xu J, Zhu B, et al. 2007. The upper ocean response to tropical cyclones in the northwestern Pacific analyzed with Argo data. Chin J Oceano Limnol, 25(2): 123–131

Maneesha K, Murty V S N, Ravichandran M, et al. 2012. Upper ocean variability in the Bay of Bengal during the tropical cyclones of Nargis and Laila. Prog Oceanogr, 106: 49–61

Mao Q, Chang S W, Pfeffer R L. 2000. Influence of large-scale initial oceanic mixed layer depth on tropical cyclones. Mon Wea Rev, 128:4058–4070

Park J J, Kwon Y-O, Price J F. 2011. Argo array observation of ocean heat content changes induced by tropical cyclones in the north Pacific. J Geophys Res, 116: C12025

Price J F. 1981. Upper ocean response to a hurricane. J Phys Oceanogr, 11:153–175

Price J F, Sanford T B, Forristall G Z. 1994. Forced stage response to a moving hurricane. J Phys Oceanogr, 24: 233–260

Robertson E J. 2003. The upper ocean salinity response to tropical cyclones [dissertation]. Rhode Island: University of Rhode Island

Sanford T B, Black P G, Haustein J R, et al. 1987. Ocean response to a hurricane Part I: observations. J Phys Oceanogr, 17(11): 2065–2083

Shay L K, Black P G, Mariano A J, et al. 1992. Upper ocean response to Hurricane Gilbert. J Geophys Res, 97: 20227–20248

Shay L K, Elsberry R L. 1987. Near-inertial ocean current response to hurricane Frederic. J Phys Oceanogr, 17:1249–1269

Shay L K, Elsberry R L, Black P G. 1989. Vertical structure of the ocean current response to a hurricane. J Phys Oceanogr, 19: 649–669

Stramma L, Cornillon P, Price J F. 1986. Satellite observations of sea surface cooling by hurricanes. J Geophys Res, 91: 5031–5035

Sun Liang, Yang Yuanjian, Fu Yunfei. 2009. Impacts of typhoons on the Kuroshio large meander: observation evidences. Atmos Ocean Sci Lett (in Chinese), 2(1): 45–50

Sun Liang, Yang Yuanjian, Xian Tao, et al. 2012. Strong enhancement of chlorophyll a concentration by a weak typhoon. Mar Ecol Prog Ser (in Chinese), 404: 39–50

Wang J-W, Han W, Sriver R L. 2012. Impact of tropical cyclones on the ocean heat budget in the Bay of Bengal during 1999: 1. Model configuration and evaluation. J Geophys Res, 117: C09020

Yang Y J, Sun L, Liu Q, et al. 2010. The biophysical responses of the upper ocean to the typhoons Namtheun and Malou in 2004. Int J Remote Sens, 31(17): 4559–4568